278

Egypt. J. Chem. **Vol. 66,** No. 6 pp. 267 - 278 (2023)

Egyptian Journal of Chemistry

http://ejchem.journals.ekb.eg/

Reduced Graphene Oxide @ Magnetite Nanocomposite and ELFEF effect on *Staphylococcus aureus* growth inhibition

Marwa M. Mostafa [1], Ibtsam M. Mohammed [1], Marwa A. Ramadan [3, 1],

Mona S. Elneklawi*[3]

1 Biophysics Department, Faculty of Science, Cairo University, Giza, Egypt
2 Department of Biomedical Equipments & Systems, Faculty of Applied Medical Sciences, October 6 University, Giza, Egypt.
3 Department of Photochemistry Photobiology, National Institute for Laser Enhanced Science (NILES) Cairo University, Cairo, Egypt.

Abstract

Background: *Staphylococcus aureus* (S. aureus) is well known as a Gram-positive pathogen that is leads to many chronic and recurrent infectious conditions such as skin infections. The microbial organism showed high resistance to some antibiotic classes. Extremely low frequency electric field (ELFEF) shows promising effect with antimicrobial activity. Nanoparticles represent a powerful tool against microbial growth.

Methods: Because of lack of ways of protection mechanisms against *S. aureus* the present study conducted first: *S. aureus* characteristics such as the growth curve, biofilm formation and antimicrobial susceptibilities and resistance mechanisms, second: the effect of reduced graphene oxide @ magnetite nanocomposite (rGO@Fe₃O₄) and extremely low frequency electric field (ELFEF) as inhibition mechanisms for *S. aureus* growth rate.

Results: *S. aureus* was affected by using rGO@Fe₃O₄ showing high growth inhibition of *S. aureus* in comparison with ELFEF which represent lower inhibitory effect than rGO@Fe₃O₄ while the emerging between ELFEF and rGO@Fe₃O₄ shows impressive results as a great factor in the inhibition of *S. aureus* and it was shown by screening its susceptibility test and biofilm formation ability.

Conclusion: The rate of *S. aureus* growth inhibition was sustained by using both rGO@Fe₃O₄ and ELFEF as antimicrobial factors for slowing down or inhibiting *S. aureus* microbial viability as a pathogen.

Keywords:

S. aureus, susceptibility test, biofilm formation, rGO@Fe₃O₄, and extremely low frequency electric field.

1. Introduction

A wide range of infectious diseases is caused by *Staphylococcus aureus* such as bacteremia, skin infections, endocarditis, pneumonia, abscesses, osteomyelitis and food poisoning [1].

Antimicrobial resistance is a great threatening for public health, due to improper utilize of anti-infective drugs in human and animal wellbeing as well as nourishment generation. Multidrug-Resistant Strains (MDR) developed due to the frequent improper use of antibiotics that leads to bacterial evolution spreading in human populations [2].

Extremely low frequency electric field direct effect was verified by many studies such as the biological functions of living organisms [3, 4]. Many studies observed cell responses caused by exposure to ELFEF [5, 6, 7, 8]. It has been considered that ELF-EF can negatively or positively inflences functional

parameters (cell development and practicality) and microorganism antimicrobial affectability depending on physical parameters of the electric field frequency connected i.e the time of the exposure, and/or the sort of microorganism utilized [9, 10, 11, 12].

The effects of ELFEFs on bacteria was investigated as an essential need to find out the chance of controlling the sensitivity of bacteria at resonance frequency [13, 14]. So, in the present study an alternative methods was used for the treatment of bacterial infections. Lately, efforts were made to control cellular activities of pathogenic characteristics and growth rate of *S. aureus* by using electric field of extremely low frequency with different frequencies [15].

The first step in the impressive developing nanotechnology field is nanomaterials because of their incredible tiny size dependent properties that

make the nanomaterials of higher priority in many areas of life necessities [16].

The eruption of COVID-19 virulent disease may further enlarging antimicrobial resistance as a result of the massive employ of antibiotics to treat patients tainted with extreme intense Respiratory disorder Coronavirus 2 (SARS-COV-2) [17, 18]. Given the quick rise of drug-resistant S. aureus but a need of antibiotic-development pipeline, elective techniques are critically required to combat antibiotic-resistant S. aureus. Recently, employing nanoparticles in technological industries is considered as one of the potential techniques to prevail over antibiotic resistance in bacteria [2].

Nanoparticles (NPs) of different metals and their oxides, such as Ag, ZnO, Fe_2O_3, Fe_3O_4, Al_2O_3, TiO_2, and CuO, inhibit antibacterial activity against Gram-negative and Gram-positive bacteria, in addition to the antifungal activity [19].

Graphene nanoparticles can be described as one of carbon nanostructures (CNSs) which include fullerene, carbon nanotubes (CNTs), graphene and diamond-like carbon (DLC) have powerful wide-range antibacterial activities. Physical abrasions and structural damage to the bacterial cell walls and cell membranes may be caused by Carbon nanostructures. Graphene nanoparticles shaped in many forms have been listed, which includes graphene oxide (GO), reduced graphene oxide (rGO), graphite and graphene nano-sheets. In general GO has potent antibacterial action. Also both size and surface area of carbon nanomaterials are essential parameters influencing their antibacterial action; that is, the improvement of the activity of interaction between GO and bacteria can be determined by rising the surface area of nanoparticles with a decrease in size [16].

Graphene nanoparticles are materials that well known with their potential of excitation because of their different applications such as in environmental energy , Nano catalysis, electrochemistry and experimented nowadays as inhibitory materials against pathogenic microorganisms such as *Staphylococcus aureus* [20].

In general, the antimicrobial performance of the nanoparticles counts on their composition, surface modification, intrinsic properties, and the type of microorganism. It has been introduced that carbon-based nanomaterials origin harm to bacterial membrane as a result of an oxidative stress [16]. Nanoparticles are taken up by cells and subsequently unleash ions intracellularly, causing cell death [21].

2. Materials and Methods:
2.1 Micro-organism growth conditions:

In this study *S. aureus* were supplied and collected from the Animal Health Research Institute (AHRI) and Central Public Health Laboratories of Army forces , the strains used in this study were *S. aureus* with ATCC 6538, lot Number 20219416 were identified using VITEK 2 compact system.

 S. aureus colonies were diluted in a sterile test tube containing 5 ml of Tryptic Soy Broth (TSB) from (Technopharmchem, Haryana, INDIA) and thoroughly mixed. Incubatation of samples were done (plue pard incubator, model PH050A, Italy) at 37°C for 18 h. The suspension was then streaked onto a Mannitol Salt Agar plate (Oxoid, Basingstoke, Hampshire, England) and incubated at 37°C for 18 h. Typical presumptive S. aureus colonies characterized with golden yellow pigmentation were then subcultured into Tryptic Soy Agar plate (TSA) and incubated at 37°C for 18 h [22].

Bacterial growth was investigated via two ways turbid metrically measuring absorbance or by counting colonies developed on agar plates (standard plate count). The bacterial growth study showed, standard calibration curve was plotted between the absorbance of the samples at 600 nm (using clean broth medium as reference sample) [23, 24] and the concentrations of the cells (CFU/mL) by plate counting method [25, 26].

- **Exposure system:**

The broth subculture was made by inoculating two colonies of *S. aureus* from TSA plate into a sterile test tube containing 5 ml of sterile tryptic soy broth (TSB), the micro-organism was then incubated at 37°C for 24 h. *S. aureus* concentrated to 0.5 McFarland standard, 20 µl of the suspended microorganism was supplied into 1.5 ml broth media tube. The study divided into three groups:

Negative control tube which represented by blank sample tube contained only 1.5 ml of TSB without organism. Positive control contained 1.5 ml TSB inoculated with the organism and the last group in this section that consist of number of test tubes containing bacterial inoculum were arranged to be exposed to different electric frequencies ranging from 0.1 Hz to 30 Hz for 30 min so as to determine growth inhibition resonance frequency, each experiment was carried out in triplicates and the average was considered. Each culture tube was incubated at 37°C for 24 h. The number of colony forming units (CFU) was used to quantify our results and was determined by plate counting technique [23]. Suitable dilutions of the bacterial cells were utilized to inoculate TSA plates. Fresh bacterial cultures were used throughout the experiments [12]. Alike conditions were set to the control samples as the exposed ones. Growth curves of bacterial cell cultures were gained by repeating measurements of optical density (OD) taken at 600

nm each hour by spectrophotometer (Spectro UV-Vis Auto UV-2602).

2.2 Synthesis of reduced graphene oxide @ magnetite nanocomposite

The surface of graphene oxide nanosheets (GO) is extremely loaded with oxygen groups as hydroxyl (-OH) and carboxylic (-COOH) groups which are active sites for nucleation and growth of magnetite nanoparticles on its surface. A solvothermal technique was employed to reduce GO to graphene and in situ change of Fe3+ ions to spherical magnetite nanoparticles in the same time forming graphene coated with magnetite nanocomposite $rGO@Fe_3O_4$. In a solvothermal technique, 0.5 g GO was done utilizing modified Hummers technique [27] exfoliated with sonication in 80 mL ethylene glycol (99.999% Sigma-Aldrich) for 1 hour at 40°C. Then, 1.6 g of ferric chloride (SigmaAldrich, MW=162.21) and 3.2 g sodium acetate (Alfa Aesar) were added with stirring at room temperature. The mixture was transferred into a Teflon-lined stainlesssteel autoclave at 200°C for 6 hours, then kept to cool to room temperature for 24 hours at room temperature. The black precipitate of $rGO@Fe_3O_4$ was created, centrifuged and washed many times with deionized water, then at final dried at 60°C in a vacuum oven to avoid the oxidation of magnetite nanoparticles. [28, 29].

- **Characterization of $rGO@Fe_3O_4$**

Spectral absorption of the prepared $rGO@Fe_3O_4$ measures were done utilizing a double beam UV-Vis-NIR spectrophotometer (Cary 5000, Agilent Technologies, Santa Clara, CA, USA). Morphology of $rGO@Fe_3O_4$ was investigated employing Transmission Electron Microscopy (TEM) with a Joel JEM JE 1200EXII transmission electron microscope (Tokyo, Japan). Few drops of dilute prepared rGO@Fe3O4 solution were deposited on carbon-coated copper grid and kept to dry at room temperature. Zeta potential measures were done by zeta sizer (Nano ZS, zeta sizer, Malvern, UK) based on the dynamic light scattering technique.

- **$S.\ aureus$ treated with $rGO@Fe_3O_4$:**

For the experimental culture, cells from stocks stored at −80 °C were propagated by sub culturing onto TSA (tryptic soy agar) plates and incubated overnight at 37 °C. From these, a loop full of the overnight bacterial growth was inoculated into sterile tubes containing 5 mL of TSB liquid media in an orbital shaker at 220 rpm and 37 °C for 16 h. Bacterial culture were diluted between 1.5×10^8 cells/ml in TSB medium or adjust the suspension to 0.5 McFarland standard then $rGO@Fe_3O_4$ suspension was made and sustained with TSB with concentration of 500 μg/ml DMSO then a sterile tubes with 5ml TSB used as blank tube, second tube inoculated with

$S.\ aureus$, third tube inoculated with $S.\ aureus$ used to be exposed to 0.8 Hz for 30 min , fourth tube contained TSB treated with $rGO@Fe_3O_4$ inoculated with $S.\ aureus$, the fifth tube contained TSB treated with $rGO@Fe_3O_4$ with $S.\ aureus$ to be exposed to 0.8 Hz for 30 min and adjust all tubes to 0.5 McFarland standard on the spectrophotometer. The growth curve was plotted by incubating with shacking over nigth each tube in 37ºc for 24 h and the OD was taken for each tube each hour for 24 hours. This experiment was done in triplicate.

2.3 Disc diffusion susceptibility test:

The CLSI disk diffusion technique 2021 was employed to investigate the antibiotic sensitivity test for all pathogenic S. aureus isolates. Incubation for 24 h in 37ºc for each isolate inoculated in Mueller–Hinton brot. The bacterial suspension was adjusted to match the 0.5 McFarland standard utilizing sterile saline solution. Spreading of each saline suspension was done onto the surface of Mueller Hinton agar plates with a sterile swab, and paper disks impregnated with antibiotics were dispensed onto the surfaces of Mueller–Hinton agar plates that were at least 24 mm apart from the center of each other utilizing a multi-disk dispenser. The diameters of the inhibition zones were measured utilizing a caliper and interpreted using standard break points accordingly to the Clinical and Laboratory Standards Institute on Antimicrobial Susceptibility Testing to categorize antibiotics as susceptible, intermediate, and resistant [30]. The bacterial isolate of $S.\ aureus$ was applied to susceptibility testing using fifteen different antibiotic discs namely (Vancomycin [VA 30μg], Tetracycline [TE 30μg], Trimethoprim–sulfamethoxazole [SXT 25μg], Imipenem [IPM 10μg] , Cefoxitine [CXN 30μg], Ciprofloxacin [CIP 5μg], Cefepime [FEP 30μg], Gentamycin [CN 10μg], and Linzolide [LNZ 30μg]. $S.\ aureus$ standardized bacterial suspension (1.5×10^8 cfu /ml) was divided into four groups (three samples per each); control, sample exposed to inhibitory frequency 0.8 Hz, sample treated with $rGO@Fe_3O_4$, sample treated with $rGO@Fe_3O_4$ at exposure frequency 0.8 Hz , The effect in each sample after the first hour of log phase in the bacterial growth curve for 30 minutes. At the end of the exposure period, samples of control and exposed groups were used to be inoculated in Mueller-Hinton agar plates. The inoculated plates were incubated at 37°C for 24 hrs. The mean diameter of each inhibition zone were measured [24].

2.4 Biofilm Formation Assay:

Biofilm interactions of $S.\ aureus$ were adjusted to OD600 = 0.5 McFarland in TSB and then further diluted 1:100 in TSB Glucose. A total of 100 μL of

_____

the bacterial suspension(s) were added to 96 wells microtiter plates .The plates were incubated for 24 h at 37 °C [31]. For each well the content was removed and washed three times after incubation with 250 µl of Phosphate Buffered Saline solution (PBS, Thermo Fisher Scientific). Staining of adherent cells was done with 0.1% crystal violet [32] solution for 15 min. then; rinsing off excess stain was done by filling the wells with sterile distilled water. The adhering dye was dissolved with 30% acetic acid. The OD of wells was investigated at 570 nm using Reader (ChroMate Awareness Technology INC) *by* [33].

• **For rGO@Fe₃O₄:**

A 96-well flat-bottom microplate (Falcon) was used for the biofilm evaluation by adding 100 µl of 10^8/ml bacteria in Tryptic soy broth (TSB). Incubation for 4 h was then performed at 37 °C in a gentle shaker (25 rpm). Afterwards, substitution of the medium was done with fresh TSB so as to get rid of cells that do not adhere to the well. Incubation of the plate was repeated at 37 °C with gentle shaking for 24 h. after that, wells were washed three times with 0.9% NaCl, and biofilms were maintained at 60 °C for 1 h. each well was supplied with Crystal violet (CV, 0.3%), 15 minutes later, excess CV was removed by putting the plate under running water. Once the plate was well dried at 60 °C, addition of 100 µl of 95% EtOH was done to the wells to liberate the CV from the biofilm. For the OD, 590 nm was the wavelength used in reading each well [34].

• **Categorization of isolates based on biofilm forming capacity**:

The following criteria were used for biofilm gradation in clinical isolates.
ODcut = ODavg of negative control + 3 × standard deviation (SD) of ODs of negative control.
1. OD ≤ ODcut = Non biofilm former (NBF)
2. ODcut < OD ≤ 2 × ODcut = Weak biofilm former (WBF)
3. 2 × ODcut < OD ≤ 4 × ODcut = Moderate biofilm former (MBF)
4. OD >4 × ODcut = Strong biofilm former.

In this study, All experiments with clinical isolates were done in quadruplet, i.e., each isolate were inoculated in 16 wells simultaneously and repeated thrice (on different days), and then, OD values were averaged and SD was calculated [35].

2.5 Dielectric Techniques:

The dielectric measurements were fulfilled for the samples in the frequency range 45Hz – 5MHz (beta dispersion range) using a Loss Factor Meter (type HIOKI 3532 LCR Hi TESTER, version 1.02, 1999, Japan), with a sample cell type PW 9510/60,

manufactured by Philips, Japan. The sample cell is formed of glass, provided two squared platinum black electrodes of 0.64 cm² area (*A*) and separated by 1 cm apart (*d*). For measurements, the cell is intrigued in a glass beaker containing the bacterial sample so as the sample suspension covers the whole volume between the cell electrodes. During the measurements, the sample in glass beaker between the electrodes was kept at a constant temperature of 24 ± 0.1°C. The capacitance (*C*) of the samples was measured at each frequency (*f*) and the resistance (*R*) was recorded. Each run was taken three times and the average was considered. The relative permittivity ($\varepsilon^{`}$), loss tangent (tan *δ*), dielectric loss ($\varepsilon^{``}$), conductivity (*σ*) and relaxation time (*τ*) of the samples were calculated for each frequency using the following relations:

$\varepsilon = Cd/\varepsilon° A$ (1)

where $\varepsilon°$ is permittivity of free space.

$\tan \delta = 1/2\pi f RC = \varepsilon^{``}/\varepsilon^{`}$ (2)

$\sigma = 2\pi f \varepsilon^{``} \varepsilon°$ (3)

$\tau = 1/2\pi fc$ (4)

where *fc* is the frequency at the midpoint of the dielectric dispersion curve [24].

2.6 Statistical analysis:

The bacterial growth data for estimation of the results were made by calculating arithmetic means and standard deviations for antibiotic susceptibility results and dielectric measurements. All these measurements have been done   and compared for exposed and unexposed samples using Student's *t* -test done and ANOVA analyses, the level of significance was set at P<0.05 [36].

3. Results:

3.1. Bacterial growth curves:

Figure 1a reveals the percentage of growth inhibition of varies frequencies ranging from 0.1Hz to 30Hz with respect to control sample containing unexposed *S. aureus*. The difference from control was significant at frequencies ranging from (0.2 to 30Hz) and for frequencies ranging from (0.8 to 1Hz) was highly significant (P < 0.0001) while for 0.1Hz was not significant at (P < 0.05). Figure 1b shows the growth curve characteristics for control and treated *S. aureus* by 0.8Hz. The difference from control was highly significant. Figure 1c integrated the change in cellular growth curve of *S. aureus* exposed to 0.8Hz, *S. aureus* sample treated with rGO@Fe₃O₄ and *S. aureus* sample treated with rGO@Fe₃O₄ exposed to 0.8Hz with respect to control sample. The difference from control was highly significant with rGO@Fe₃O₄ and rGO@Fe₃O₄ exposed to 0.8Hz electric field.
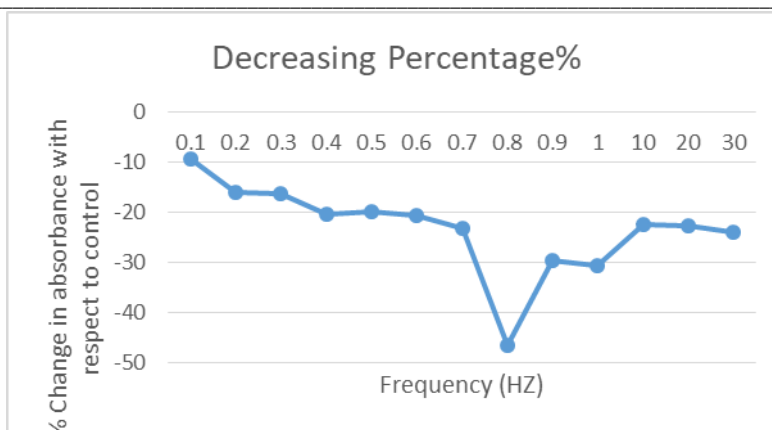
_____

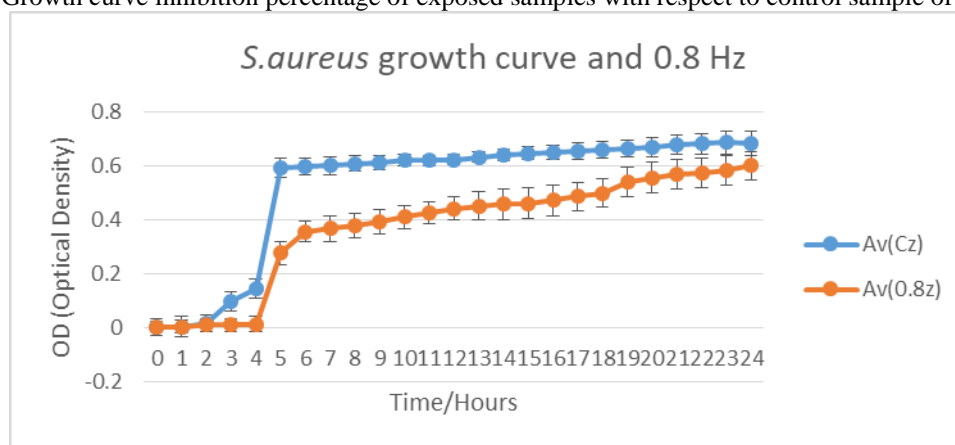Fig.1a: Growth curve inhibition percentage of exposed samples with respect to control sample of *S. aureus*

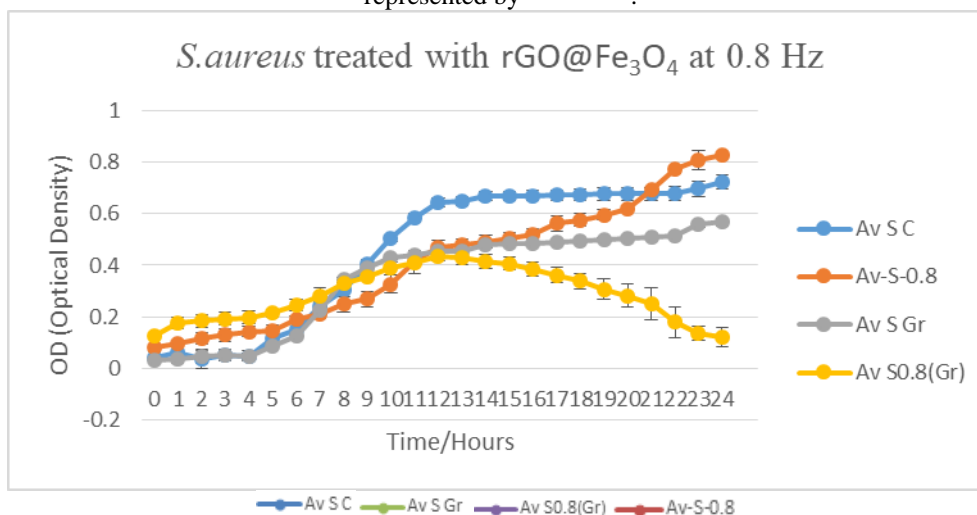Fig.1b: Growth curve characteristics for control represented by ▬●▬ Av(Cz) and treated *S. aureus* by 0.8 Hz represented by ▬●▬ Av(0.8z) .

Fig.1c: *S. aureus* samples comparison between *S. aureus* control sample represented by, *S. aureus* exposed to 0.8Hz represented by , *S. aureus* treated with rGO@Fe₃O₄ showed by and *S. aureus* treated with rGO@Fe₃O₄ exposed to 0.8Hz showed by .

▬●▬ Av S C

3.2 Synthesis of rGO@Fe₃O₄ and its characterization

Confirmation of successful preparation of rGO@Fe₃O₄ was obtained with The UV-visible- NIR optical absorbance spectra (Figure 2a), at about 260

nm characteristic peak and the solution has high background dark color with a broad absorption band from UV, visible and NIR spectral region.

After solvothermal reduction, layered structures were displayed from graphene sheets and became very thin

and clear vision of the folding nature was obsereved. The graphene sheets are exfoliated and cannot restack any more, Fig.2b shows the typical TEM image of rGO@Fe$_3$O$_4$ nanocomposite, the Fe$_3$O$_4$ spheres are uniformly decorated and firmly anchored on the wrinkled graphene layers with a high density and serve as a stabilizer separate graphene sheets against the aggregation.

The surface of rGO@Fe$_3$O$_4$ is mostly negatively charges due to coating with poly ethylene glycol which was noticeably concluded from zeta potential measurements by DLS, figure 2c The average surface potential was -22.2 mV allow it to creat steady solution in water and assist its absorption by cellular membrane.

3.3 Bacterial susceptibility test analysis:

The antibiotic susceptibility test results for control, exposed to 0.8 Hz, and treated samples with rGO@Fe$_3$O$_4$ are detailed in Table 1. Significant difference between unexposed and exposed samples

and treated samples with rGO@Fe$_3$O$_4$ were observed, figure 2 demonstrates the comparison between the four different samples for each antibiotic used.

3.4. Biofilm Measurements:

To confirm the impact of 0.8Hz ELFEF on the *Staphylococcus aureus* biofilm formation, bacterial cultures in microtiter plates were exposed for 30 min, and treated samples with rGO@Fe$_3$O$_4$ compared to the relative non-exposed controls. The results revealed the inhibition of the biofilm activity at 0.8Hz as shown in Table 3.

3.5. Dielectric Measurements:

Properties of molecules are affected majorly by the dielectric behavior of microorganism such as *S. aureus*, the following dielectric data, shown in Table2 shows the differences of relative permittivity and conductivity between control and exposed microorganism at inhibitory frequency of 0.8 Hz, treated microorganism with rGO@Fe$_3$O$_4$.
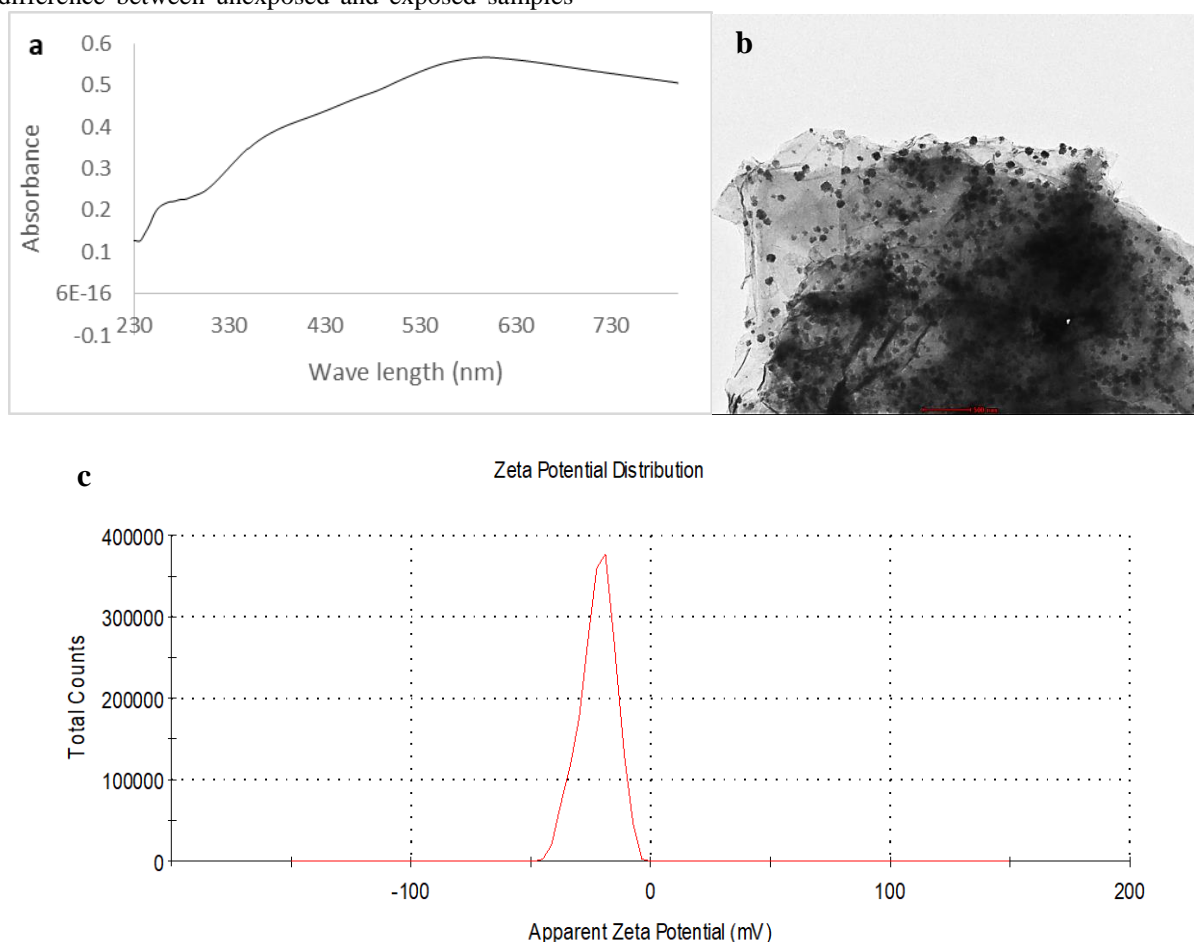
Figure 2: rGO@Fe$_3$O$_4$ (a) UV-visible absorption curve (b) TEM image (magnification 500 nm) (c) Zeta potential.
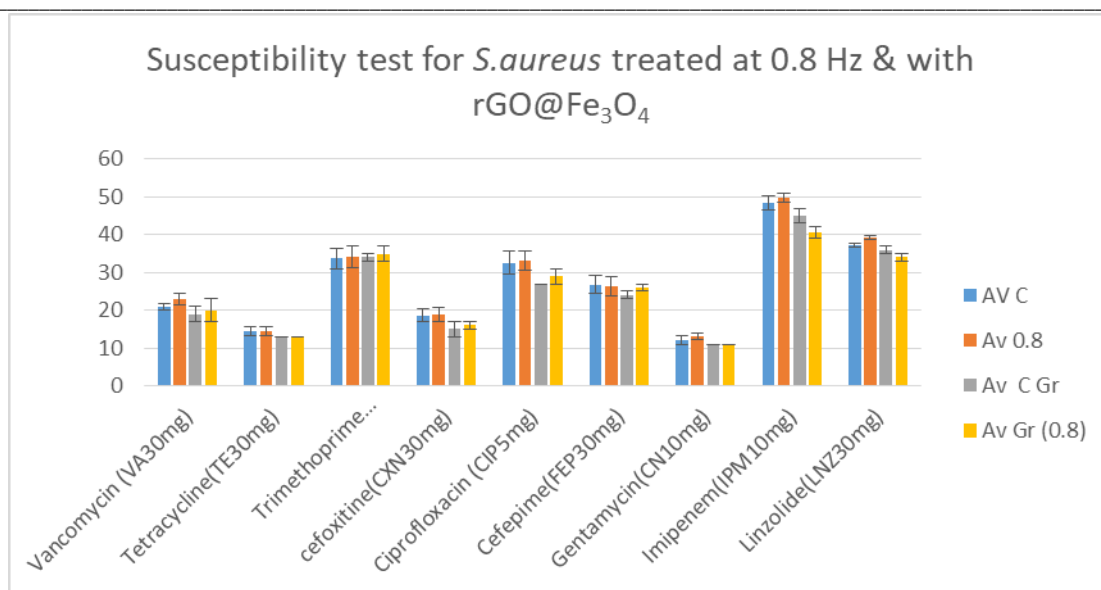
▪ Av Ag0.8 .

Fig.2 The zone diameter difference between *S. aureus* control sample represented by ■ AV C , exposed sample at 0.8Hz represented by ■ Av 0.8 and treated samples with rGO@Fe$_3$O$_4$ represented by ■ Av C Gr and treated sample with rGO@Fe$_3$O$_4$ exposed at 0.8Hz represented by ■ Av Gr (0.8) .

Table 1: the mean inhibition zone diameter (mm) and percentage of inhibition with respect to control sample of different antibiotic agents for the control, exposed and treated samples with rGO@Fe$_3$O$_4$.

Antibiotic Disc	Average control	0.8 Hz inhibition percentage%	0.8 Hz Zone Diameter	rGO@Fe$_3$O$_4$ inhibition percentage%	rGO@Fe$_3$O$_4$ Zone D	rGO@Fe$_3$O$_4$ at 0.8Hz inhibition percentage%	rGO@Fe$_3$O$_4$ at 0.8 Hz
Cell wall inhibitor Vancomycin (VA 30mg)	**S** 21± 0.836	9.50%	**S** 23±1.51	-9.50%	**I** 19±2	-4.76%	**I** 20±3
Protein Synthesis Inhibition (Anti-30S ribosomal subunit) (TE 30mg)	**I** 14.4± 1.07	0%	**I** 14.4±1.07	-9.72%	**R** 13±0	-9.72%	**R** 13±0
Folic acid Synthesis Inhibitors (sxt 25mg)	**S** 33.8± 2.727	1.10%	**S** 34.2±2.85	0.50%	**S** 34±1	3.55%	**S** 35±2
Cephalosporins (2nd generation) (CXN 30mg)	**R** 18.6± 1.720	1%	**R** 18.8±1.9	-19.35%	**R** 15±2	-13.97%	**R** 16±1
DNA Synthesis Inhibitors (Fluoroquinolones-2nd generation) (CIP 5mg)	**S** 32.6± 2.993	1.80%	**S** 33.2±2.53	-17.70%	**S** 27±0	-11.04%	**S** 29±2
Cephalosporins (4th generation) (FEP 30 mg)	**I** 26.8± 2.374	-1.49%	**I** 26.4±2.56	-10.40%	I 24±1	-2.98%	**I** 26±1
Protein Synthesis Inhibition (Aminoglycosides) (CN 10mg)	**I** 12.2± 1.2	6.55%	**I** 13±0.89	-9.83%	**R** 11±0	-9.80%	**R** 11±0

Cell wall inhibitors (Carbapenems) (IPM 10mg)	S 48.4± 1.72	2.80%	S 49.8±1.24	-7.02%	S 45±2	-16.32%	S 40.5±1.5
Anti-50S ribosomal subunit (LNZ 30mg)	S 37.2± 0.583	5.37%	S 39.2±1.095	-0.50%	S 36±1	-8.60%	S 34±1

Note: S refers to Susceptible, I refers to Intermediate & R refers to Resistance.

Table.3: Biofilm Mean for control sample, exposed sample to 0.8Hz and treated samples with rGO@Fe$_3$O$_4$.

S. aureus samples	OD cut off	Biofilm Mean	Biofilm SD
S. aureus control sample	1.797 *	1.98*	±0.01
S. aureus treated with 0.8 Hz	2	1.76	±0.078
S. aureus treated with rGO@Fe$_3$O$_4$	2.31	2.14	±0.09
S. aureus treated with rGO@Fe$_3$O$_4$ & 0.8 Hz	2.58	2.27	±0.046

Weak Biofilm (*)

The curves of dielectric relaxation for *s. aureus* groups ar demonstrated in figure.4 (a, b, and c). The findings show a dielectric dispersion in the frequency range indicated. The data also showed an elevation in the electrical conductivity which is accompanied with any drop off in the dielectric loss in the sample. The values of η, and σ were obtained from the curves for all samples from all groups as given in Table (2), the difference is not significant (NS) (p > 0.05) while the difference is highly significant (HS) (P<0.0001)
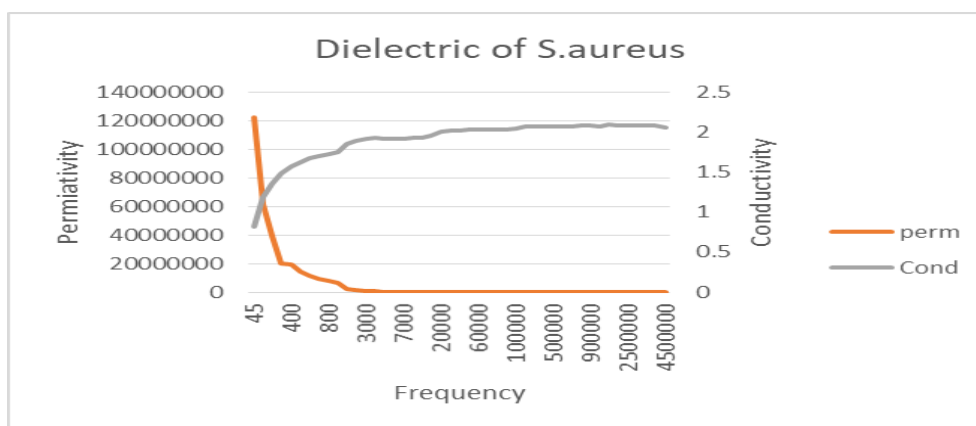

Fig.4a Dielectric of control sample in which conductivity represented by ——Cond s(C) and permittivity represented by —— perm .
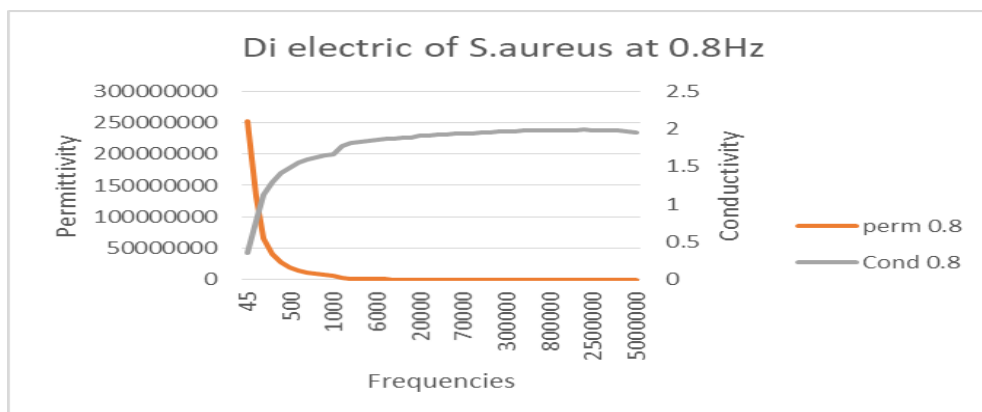

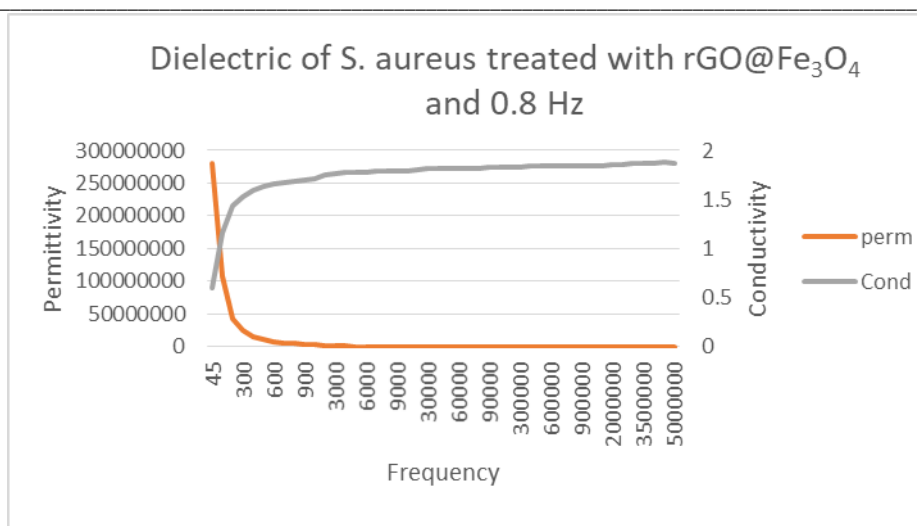Fig.4b Dielectric of *s. aureus* exposed sample to 0.8Hz

Fig.4c Dielectric of *S. aureus* treated sample with rGO@Fe$_3$O$_4$ and exposed to 0.8 Hz

Table 2. Dielectric parameters for control sample, samples exposed to 0.8 Hz for 30 min, and treated sample with rGO@Fe$_3$O$_4$ and exposed to 0.8 Hz.

Experimented Samples	Dielectric increment $\Delta\varepsilon(\varepsilon\circ - \varepsilon\infty)$	Conductivity $\sigma \times 10{-2}$ at 3 MHz (s/m)
Control	105932387005518±5.9	2.077793 ± 0.00852
Treated sample with 0.8 Hz	252436305±4.2×10^{-6}	1.984371±0.011
Treated sample with rGO@Fe$_3$O$_4$ at 0.8 Hz	280331755.9±0.0	1.86±0.0

4. Discussion and Conclusion:

The main goal of this study is to inspect extremely low frequency also revealing the impact of adding Nano particles as reduced Graphene Oxide to Staphylococcus aureus during the exposure that affects the Staphylococcus aureus growth. This technique was used to detected the difference between the inhibitory effect of extremely low electric frequency 0.8Hz on Staphylococcus aureus and the inhibitory effect of 0.8Hz adding to Nanoparticles such as Graphene Oxide. The results of the inhibitory frequency and Nanoparticles used may lead to distinguish changes in molecular structure of the microorganism at the log phase that caused to affect its cellular division, as the growth curves of the exposed Staphylococcus aureus differ from the control sample starting from the log phase as showed in fig.9c. there is a destructive resonance interference of the applied square wave at 0.8 Hz for *S.aureus* with the bioelectric signals produced along the microbial cellular division. These applied waves could be the reason for the ions to deflect from their regular way of cellular division, and then lead the process to deteriorate. The biological cellular membrane is composed of phospholipids bilayers molecules imbedded in between protein molecules (intrinsic and extrinsic), the effect of exposures to resonance frequency 0.8Hz may cause the disturbance of the intermolecular forces between the macromolecules forming the cellular membrane [37]. Analysis of the influence of graphene on the morphology and ultrastructure of the cell showed damage to the bacterial structure cell wall and cell membrane treated with rGO. Bacterial cell can suffer from disorders of membrane integrity that can prevent respiration, transport across the membrane and osmotic balance [38]. Our findings are in agreement with the findings of earlier investigations reporting the inhibitory effects of ELF and reduced Graphene Oxide Nanoparticles on growth and viability of Staphylococcus aureus and dependence of this effect on exposure time [39, 40]. This results lead to a conclusion that permittivity of microorganism cell membrane transformed leading to changes in inner cell constituents, while the changes occurred in the log phase stage. Indicating that adding Graphene Oxide Nanoparticles to microorganism during exposure to 0.8Hz may cause changes to the cell membrane permittivity due to exposure by the inhibitory frequencies including the influence of reduced Graphene Oxide Nanoparticles as in Figs 11a,11c. The antibacterial action of rGO and other carbon-based nanomaterials in studied investigating the impact of exposure time and concentration [40]. The antibacterial activity of GO susceptibility test specially with Trimethoprime sulfamethoxazole

(sxt25mg). Antibiotic susceptibility test concerned with inhibitors of cell wall synthesis showed an observed difference in diameterzone confirming the effect of inhibitory frequency combined with rGO Nanoparticles on cell wall this fact agreed with [41]. The construction and evaluation for Nanoantibiotics in the inhibition of bacterial growth was confirmed, even in planktonic or sessile forms. Incapability of antimicrobial agents to infiltrate into the biofilm network, leading to the progress of resistant microbial strains, may be defeated via the application of nanostructures exhibiting antibiofilm action [42, 43]. The prospective of antibacterial applications of graphene-based nanocomposites has remarkable considerable employments [44, 45]. rGO Nanoparticles showed a destructive effect on biofilm formation of Staphylococcus aureus and this fact in agreement with [46, 47].

There is a noticeable change of exposed S. aureus samples at 0.8Hz exposed for 30min also there is a significant decrease in s. aureus activity treated with rGO@Fe_3O_4 exposed to ELFEF 0.8Hz than the treated sample with rGO@Fe_3O_4 only, and this was shown clearly with susceptibility test and biofilm test.

Conflict of interest

We certify that there is no conflict of interest with any financial organization regarding the material discussed in the manuscript.

References:

1. Ahmed Haiam M., Rageh Monira M., Mohamad Ebtesam A. (2022). Curcumin provides skin Protection against UV radiation. Egypt. J. Chem. In press.
2. Haibo Wang, Minji Wang , Xiaohan Xu, Peng Gao, Zeling Xu, Qi Zhang, Hongyan Li, Aixin Yan ,Richard Yi-Tsun Kao & Hongzhe Sun., 2021. Multi-target mode of action of silver against Staphylococcus aureus endows it with capability to combat antibiotic resistance NATURE COMMUNICATIONS | (2021) 12:3331 | https://doi.org/10.1038/s41467-021-23659-y.
3. A.Inhan_Garip,B.Aksu,Z.Akan,D.akakin,A.N.oz aydin, and T.San., 2008. Effects of extremely low frequency electromagnetic fields on growth rate and morphology of bacteria, International Journal of Radiation Biology vol,87,No.12,pp.1155_1161.
4. Y.D.Alipov,I.Y.Belyaev, and O.A.Aizenberg., 1994 Systemic reaction of Escherichia coli cells to weak electromagnetic fields of extremely low frequency, Bioelectrochemistry and Bioenergetics,vol.34,No.1,pp.5_12.
5. Mohamad, E.A., Ahmed, K.A. & Mohammed, H.S. (2022) Evaluation of the skin protective effects of niosomal-entrapped annona squamosa against UVA irradiation. Photochem Photobiol Sci.
6. Ali Abeer A., El-Gebaly Reem H., Mohamad Ebtesam A. (2022). N-Acetylcysteine encapsulated niosomes as antitumor nanoparticles. Egypt. J. Chem. In press.
7. E.S. A.Gaafar, M.S. Hanafy, E.T. Tohamy, and M.H.Ibrahim., 2006 Stimulation and control of E.Coli by using an extremely low frequency, in vivo Electromagn Biol Med. 24: 9-12.
8. Perez, V.H., Reyes, A.F., Justo, O.R., Alvarez, D.C. and Alegre, R.M. (2007) Bioreactor coupled with electromagnetic field generator: effects of extremely low frequency electromagnetic fields on ethanol production by Saccharomyces cerevisiae. Biotechnology Progress, Vol. 23, 1091-1094.
9. I.V.Babushkina,V.B. Borodulin,N.A.Shmetkova et al., 2005 The influence of alternating magnetic field on Escherichia coli in vitro yet not through *agr* regulation and Sarne De Vliegher1 Toledo‑Silva *et al. Veterinary Res 52:114*.
10. I.Belyaev., 2011 Toxicity and SOS_response to ELF magnetic fields and nalidixic acid in E.coli cells, Mutation Research,vol.722,No.1,pp.56_61.
11. L.Cellini,R.Grande,E.DiCampli et al., 2008 Bacterial response to the exposure of 50Hz electromagnetic fields, Bioelectromagnetics,vol.29,No.4,pp.302_311.
12. Ali F. M., El_Khatib A. M., Sabry S. A., Abo_Neima S. E., Motaweh H. A., 2013 CONTROL OF STAPHYLOCOCCUS AUREUS GROWTH BY ELECTROMAGNETIC THERAPY vol 155 No.6 *Natural sciences*.
13. Liang Z, Cheng Z, Mittal G., 2006. Inactivation of spoilage microorganisms in apple cider using a continuous flow pulsed electric field system. LWT. Food Science and Technology 39: 351–357. ISSN 0023-6438, https://doi.org/10.1016/j.lwt.2005.02.019.

14. Ayse IG, Burak A, Zafer A, Dilek A, Nilufer OA, Tangul S (2011).Effect of extremely low frequency electromagnetic fields on growth rate and bacterial cells, Pharmaceutical Chemistry Journal,vol.39,no.8,pp.398_400.

15. Ali, Fadel & Gawish, Azza & Osman, Massarat & Abdelbacki, Ashraf & Hamdi, Amira. (2012). Control of salmonella activity in rats by pulsed elf magnetic field (in vivo study). Journal of International Dental and Medical Research. 5 (2) 2012. pp. 129-135.

16. Maleki Dizaj S, Mennati A, Jafari S, Khezri K, Adibkia K. Antimicrobial activity of carbon-based nanoparticles. Adv Pharm Bull. 2015 Mar;5(1):19-23. doi: 10.5681/apb.2015.003. Epub 2015 Mar 5. PMID: 25789215; PMCID: PMC4352219.

17. Editorial: Antimicrobial resistance in the age of COVID-19. Nat. Microbiol. 5, 779 (2020).

18. Rawson, T. M., Ming, D., Ahmad, R., Moore, L. S. P. & Holmes, A. H. , 2020Antimicrobial use, drug-resistant infections, and COVID-19. Nat. Rev. Microbiol. 18, 409–410.

19. Gudkov, S.V.; Burmistrov, D.E.; Serov, D.A.; Rebezov, M.B.; Semenova, A.A.; Lisitsyn, A.B. Do Iron Oxide Nanoparticles Have Significant Antibacterial Properties?.Antibiotics 2021, 10, 884.

20. Sanjay R.Thakare, Vivek R.Mate, KalyaniUrkude, and Sandeep B.Gawande. 2020 Graphene-TiO2-polyaniline nanocomposite: A New green and efficient catalyst as a alternative for Nobel metal and NaBH4 induced the reduction of 4-Nitro phenol. FlatChem 22.

21. Hou, X., Zaks, T., Langer, R. *et al.* Lipid nanoparticles for mRNA delivery. *Nat Rev Mater* 6, 1078–1094 (2021). Doi.org/10.1038/s41578-021-00358-0.

22. Fikirte Lemma, Haile Alemayehu, Andrew Stringer and Tadesse Eguale, 2021, Prevalence and Antimicrobial Susceptibility Profile of Staphylococcus aureus in Milk and Traditionally Processed Dairy Products in Addis Ababa, Ethiopia, Hindawi BioMed Research International Volume 2021, Article ID 5576873, 7 pages https://doi.org/10.1155/2021/5576873.

23. Atlas R. Principles of Microbiology. Mosby-Year book,INC,1995.

24. Fadel M. Ali, Reem H. Elgebaly, Mona S. Elneklawi, and Amal S. Othman. 2016 Role of duty cycle on Pseudomonas aeruginosa growth inhibition mechanisms by positive electric pulses" Bio-medical Materials and Engineering 27(2-3):211-225, DOI:10.3233/BME-161577.

25. Demicheli M, Goes A, Ribeiro A., 2007 Ultrastructural changes in Paracoccidioides brasiliensis yeast cells attenuated by gamma irradiation. J.Compil, 50: 397–402.doi: 10.1016/j.msec.2019.02.027. doi: 10.4103/jgid.jgid_91_16.

26. Sahar E.Abo-Neima1, Yasser I.Khedr , Hussein A.Motaweh, Metwaly M.K and Ahmed Elhoseiny,2016, Control the metabolic activities of E.coli and S. aureus bacteria by Electric Field waves at Resonance Frequency in vitro study, vol 52 research gate.

27. Samah A Loutfy, Taher A. Salaheldin, Marwa A Ramadan, et al., Synthesis, Characterization and Cytotoxic Evaluation of Graphene Oxide Nanosheets: In Vitro Liver Cancer Model. asian pacific journal of cancer prevention, 2017. 18: p. 955-961.

28. Salaheldin, T.A., S.A. Loutfy, M.A. Ramadan, IR-enhanced photothermal therapeutic effect of graphene magnetite nanocomposite on human liver cancer HepG2 cell model. International journal of nanomedicine, 2019. 14: p. 4397-4412.

29. Lunhong Aia, Chunying Zhangb, and Z. Chena, Removal of methylene blue from aqueous solution by a solvothermal-synthesized graphene/magnetite composite. Hazardous Materials, 2011. 192: p. 1515– 1524.

30. Abdelaziz AR, Tahoun A, El-Sharkawy H, Abd El-Salam MM, Alorabi M, El-Shehawi AM, El Meghanawy RA, Toukhy EE, Abd El-Salam AM, Sorour SSG. Overview on *Cryptosporidium bovis* and Its Effect on Calves in Some Governorates in Egypt. J Trop Med. 2022 May 31;2022:4271063. doi: 10.1155/2022/4271063. PMID: 35686207; PMCID: PMC9173906.

31. Toledo-Silva B, de Souza FN, Mertens K, Piepers S, Haesebrouck F, De Vliegher S. Bovine-associated non-aureus staphylococci suppress Staphylococcus aureus biofilm dispersal in vitro yet not through agr regulation. Vet Res. 2021 Sep 3;52(1):114. doi: 10.1186/s13567-021-00985-z. PMID: 34479647; PMCID: PMC8414718.

32. Da Silva FAG Jr, Alcaraz-Espinoza JJ, da Costa MM, de Oliveira HP. Low intensity electric field inactivation of Gram-positive and Gram-negative bacteria via metal-free polymeric composite. Mater Sci Eng C Mater Biol Appl. 2019 Jun;99:827-837. doi: 10.1016/j.msec.2019.02.027. Epub 2019 Feb 11. PMID: 30889757.

33. Samuel Bucko, Anna Čuvalová, Ján Labun, Ján Zbojovský, Dobroslava Bujňáková, Vladimír Kmeť. 2020 "MODULATION OF *STAPHYLOCOCCUS AUREUS* BIOFILM BY

ELECTROMAGNETIC RADIATION" JOURNAL OF MICROBIOLOGY, BIOTECHNOLOGY AND FOOD SCIENCES. vol. 9, no. 5. DOI:10.15414/jmbfs.2020.9.5.1020-1022 .

34. Valentina Gargiulo, Brigida Alfano, Roberto Di Capua, Michela Alfé, Mykhailo Vorokhta, Tiziana Polichetti, Ettore Massera, Maria Lucia Miglietta, Chiara Schiattarella, *and* Girolamo Di Francia. 2018 Graphene-like layers as promising chemiresistive sensing material for detection of alcohols at low concentration. Journal of Applied Physics 123, 024503 https://doi.org/10.1063/1.5000914.

35. Singh AK, Prakash P, Achra A, Singh GP, Das A, Singh RK. Standardization and Classification of *In vitro* Biofilm Formation by Clinical Isolates of *Staphylococcus aureus*. J Glob Infect Dis. 2017 Jul-Sep;9(3):93-101. doi: 10.4103/jgid.jgid_91_16. PMID: 28878520; PMCID: PMC5572203.

36. Fadel M. Ali, Hala M. Ahmed, Nashwa A. Ahmed and Mona S. Elneklawi. (2018) Evaluation of the Effect of Extremely Low-Frequency Electromagnetic Fields on the Growth of Escherichia coli. International Journal of Scientific & Engineering Research 9(7):1060-1079. ISSN 2229-5518

37. Fadel M. Ali, Shaimaa A. Mohamed, Ashraf Abdelbacki, and Amira Hamdi. 2014. Inhibition of Salmonella typhi Growth Using Extremely Low Frequency Electromagnetic (ELF-EM) Waves at Resonance Frequency. Journal of Applied Microbiology 117(2): p. 358-365.

38. Sławomir Jaworski , Barbara Strojny-Cie´slak , MateuszWierzbicki , Marta Kutwin , Ewa Sawosz ,Maciej Kamaszewski , Arkadiusz Matuszewski , Malwina Sosnowska , Jarosław Szczepaniak ,Karolina Daniluk , Agata Lange , Michał Pruchniewski , Katarzyna Zawadzka , Maciej Łojkowski , and Andre Chwalibog , 2021Comparison of the Toxicity of Pristine Graphene and Graphene Oxide, Using Four Biological Models, Materials, vol.14, No4250.

39. Abdelmoneam Eman A, Rageh Monira M., Mohamad Ebtesam A. (2022). Antitumor efficacy of Curcumin nanoparticles. Egypt. J. Chem. In press.

40. Li, R.; Mansukhani, N.D.; Guiney, L.M.; Ji, Z.; Zhao, Y.; Chang, C.H.; French, C.T.; Miller, J.F.; Hersam, M.C.; Nel, A.E.; et al. Identification and Optimization of Carbon Radicals on Hydrated Graphene Oxide for Ubiquitous Antibacterial Coatings. ACS Nano 2016, 10, 10966–10980.

41. M. Olivi & M. Alfè & V. Gargiulo & F. Valle & F. Mura & M. Di Giosia & S. Rapino & C. Palleschi & D. Uccelletti & S. Fiorito, 2016, Antimicrobial properties of graphene-like nanoparticles: coating effect on Staphylococcus aureus, J Nanopart Res, vol: 18, pp: 358.

42. María Paulina Romero, Valeria Spolon Marangoni, Clara Gonçalves de Faria1,Ilaiali Souza Leite, Cecília de Carvalho Castro e Silva, Camila Marchetti Maroneze,Marcelo A. Pereira-da-Silva1, Vanderlei Salvador Bagnato1 and Natalia Mayumi Inada1 2020, Graphene Oxide Mediated Broad-Spectrum Antibacterial Based on Bimodal Action of Photodynamic and Photothermal Effects, Frontiers in Microbiology ,vol 10, No 2995.

43. Li J, Wang G, Zhu H, Zhang M, Zheng X, Di Z, Liu X, Wang X (2014) Antibacterial activity of large-area monolayer graphene film manipulated by charge transfer. Sci Rep 4:4359.

44. Huh AJ, Kwon YJ (2011) BNanoantibiotics^: a newparadigmfor treating infectious diseases using nanomaterials in the antibiotics resistant era. J Control Release 156(2):128–145.

45. Ansari AM, Khan HM, Khan AA, Cameotra WS, Pal R (2013)Antibiofilm efficacy of silver nanoparticles against biofilm of extended spectrum β-lactamase isolates of Escherichia coli and Klebsiella pneumoniae. Appl Nanosci 4(7):859–868.

46. Yang K, Li Y, Tan X, Peng R, Liu Z (2012) Behavior and toxicity of graphene and its functionalized derivatives in biological systems. Small vol.9, No(9–10), pp.:1492–1503.

47. Hegab HM, ElMekawy A, Zoua L, Mulcahy D, Saint CP, Ginic-Markovic M (2016) The controversial antibacterial activity of graphene-based materials. Carbon 105:362–376Sihem, L.; Hanine, D.; Faiza, B.,2020, Antibacterial Activity of _-Fe2 O3 and _-Fe2O3@ Ag Nanoparticles Prepared by Urtica Leaf Extract. Nanotechnol. Russ.,vol 15,pp. 198–203